https://doi.org/10.5194/egusphere-2024-4166
Preprint. Discussion started: 23 January 2025

Drivers of the spatiotemporal distribution of dissolved nitrous oxide and air-sea exchange in a coastal Mediterranean area

Susana Flecha[1], Mercedes de la Paz[2], Fiz Fernández Pérez[2], Núria Marbà[3], Carlos Morell[3], Eva Alou-Font[4], Joaquín Tintoré[3,5] and Iris E. Hendriks[3]

[1]Instituto de Ciencias Marinas de Andalucía (ICMAN-CSIC), Puerto Real, Cádiz, Spain.
[2]Instituto de Investigaciones Marinas (CSIC), Vigo, Spain
[3]Mediterranean Institute for Advanced Studies (CSIC-UIB), Esporles, Spain
[4]King Abdullah University of Science and Technology (KAUST), Thuwal, Kingdom of Saudi Arabia.
[5]Balearic Islands Coastal Observing and Forecasting System (SOCIB), Palma, Spain

Correspondence to: Susana Flecha (susana.flecha@csic.es)

Abstract. Among the well-known greenhouse gases (GHG), nitrous oxide (N_2O) is the third most impactful, possessing a global warming potential approximately 300 times greater than carbon dioxide (CO_2) over a century. The distribution of N_2O from aquatic environments exhibits notable spatial and temporal variations, and emissions still remain inadequately constrained and underrepresented in global N_2O emission inventories, particularly from coastal zones. This study focuses on the N_2O levels and air-sea fluxes in the Balearic Islands Archipelago coastal waters in the Western Mediterranean Basin. Data were gathered between 2018 and 2023 at three coastal monitoring stations: two in the highly inhabited island of Mallorca and the third in the well-preserved National Park of the Cabrera Archipelago. Seawater N_2O concentrations varied from 6.5 to 9.9 nM, with no significant differences detected across the sites. The average air-sea fluxes were estimated to range from -0.3 to 0.6 µmol m^{-2} d^{-1}, indicating that the study areas generally functioned as weak N_2O sources. A consistent seasonal pattern was noted over the study period. Machine learning analysis indicated that seawater temperature was the primary factor influencing N_2O concentrations, with lesser contributions from chlorophyll levels and salinity.

1 Introduction

Nitrous oxide (N_2O) is a potent greenhouse gas (GHG) with 300 times higher warming potential per mole than carbon dioxide (CO_2) on a 100-year time scale (Solomon et al., 2007). Atmospheric N_2O levels have increased by more than 18% since preindustrial times and increased by 332 ppb between 2011 and 2019 (Masson-Delmotte et al., 2021). The ocean N_2O budget is highly sensitive to climate changes and significantly influences the climate system. Variations in temperature, ocean circulation, and biological activity can alter the production and release of N_2O from the oceans. In turn, the concentration of nitrous oxide in the atmosphere affects global warming and climate patterns, creating a feedback loop between the oceanic processes and the climate system. Marine N_2O sources represent a third part of the natural emissions to the atmosphere, yielding a net source of 3.5 (2.5-4.7) Tg N yr^{-1} without considering the coastal contribution (Tian et al., 2024). N_2O is produced mainly by nitrification and denitrification pathways (Freing et al., 2012). The nitrogen cycle is one of the most complex regulating factors of primary production, highly dependent on dissolved oxygen concentration and the prevailing redox regime (Codispoti, 2010). In coastal environments, there is considerable variability in the nitrogen cycle, where land-derived solid nutrient inputs, coastal upwelling events, and complex biogeochemical processes play

https://doi.org/10.5194/egusphere-2024-4166
Preprint. Discussion started: 23 January 2025

important roles (Doney, 2010), contributing significantly to the spatiotemporal variability of the N_2O (Nevison et al., 1995). In estuarine and coastal waters, the effects of climate change may be more severe, such as ocean acidification (OA, Carstensen and Duarte, 2019), which also stimulates the generation of N_2O (Wan et al., 2023; Zhou et al., 2023).

Despite the necessity for a better understanding of atmospheric and oceanic inventories of non-CO_2 GHGs to provide realistic and accurate models for future scenarios, there are limited open ocean and coastal monitoring time series networks compared to CO_2 (Bakker et al., 2014; de la Paz et al., 2015; Farías et al., 2007; Ma et al., 2019; Wilson et al., 2017).

The Mediterranean Sea is a semi-enclosed basin surrounded by highly sensitive coastal zones particularly vulnerable to human activities. Factors such as high population density, widespread urbanization, and intensive agriculture have escalated risks of pollution and habitat degradation in the region. Due to its distinct biogeochemical and hydrodynamic features, this basin has been identified as a "hotspot" for climate change research (Giorgi, 2006). The impacts of global warming and extreme weather events are expected to be more severe in the Mediterranean compared to other oceanic regions (Giorgi, 2006; Giorgi and Lionello, 2008; Masson-Delmotte et al., 2021). Despite representing just 0.82% of the global ocean surface, the Mediterranean hosts 4-18% of the world's marine biodiversity, including numerous endemic species (Bianchi and Morri, 2000; Mouillot et al., 2011). Rising temperatures and ocean acidification threaten the biodiversity of the region (Micheli et al., 2013). Additionally, anthropogenic pressures along the Mediterranean coast have intensified due to rapid population growth and economic activities. In the Western Mediterranean, high tourism and coastal development levels have left only a small fraction of the coastline in a natural state, with even fewer areas under protection (EEA, 1999).

The Balearic Islands Archipelago, located in the Western Mediterranean, consists of Mallorca, Menorca, Ibiza, and Formentera, with a combined coastline of 1,723 km. Renowned as a major European tourist destination, tourism contributes approximately 45% of the total Gross Domestic Product of the archipelago. Visitor numbers have risen dramatically over the past century, reaching nearly 18 million in 2023 (Institut d'Estadística de les Illes Balears, Spain), compared to a resident population of around 1.2 million. Coastal ecosystems in the Balearic Islands are essential for the local economy. Meadows of the endemic seagrass *Posidonia oceanica* extend across depths of up to 45 m in the Balearic Sea, providing critical ecosystem services such as carbon sequestration (Duarte et al., 2005), oxygen production (Hendriks et al., 2022), biodiversity support, coastal erosion prevention, sediment stabilization, and water transparency (Barbier et al., 2011). However, these ecosystems face mounting pressure from recreational activities and other anthropogenic impacts.

Given the increasing threats to these ecosystems, understanding the relationship between anthropogenic pressures and greenhouse gas emissions, particularly nitrous oxide (N_2O), has become urgent. The absence of long-term N_2O datasets in the Mediterranean Sea, combined with the uncertainties surrounding current emissions estimates, underscores the importance of assessing coastal areas with varying human impacts. These evaluations are essential for improving coastal N_2O emissions estimates and refining global ocean N_2O budgets.In this study, we evaluate the spatial and temporal variability of N_2O concentrations in surface

https://doi.org/10.5194/egusphere-2024-4166
Preprint. Discussion started: 23 January 2025

waters and the air-sea exchange in the coastal area of the Balearic Islands Archipelago and estimate the potential drivers of the observed N_2O variability. We focused on three different sites in the coastal zone: a highly impacted site and a medium-impacted site, both located near the island of Mallorca and a pristine station in the Cabrera National Park Archipelago.

2 Methods

2.1 Study area

We collected physicochemical and biogeochemical parameters from the three stations located in the Balearic Sea in the Western Mediterranean Basin (Fig. 1A) integrated into the Balearic Ocean Acidification Time Series (Flecha et al., 2022).

Two sampling sites are fixed monitoring stations with deployed autonomous sensors. The first is located in the bay of Palma (BP: 39.492848ºN, 2.700405ºE, over a bottom depth of ~30 m, Figure 1B) and is part of the fixed monitoring station belonging to the Balearic Islands Coastal Observing and Forecasting System (Tintoré et al., 2019, 2013- SOCIB; https://www.socib.es/). Temperature (ºC) and salinity (PSU) were obtained from the SOCIB buoy sensors; see Tintoré and Casas (2022) for sensor details. Additionally, a MiniDot sensor (PME, Inc©) recorded DO hourly. The manufacturer accuracy of the DO measurements was ± 5%.

The second fixed monitoring station is located in the Bay of Santa Maria (Fig. 1B) in the Cabrera Archipelago National Park (CA: 39.151395º N, 2.950823ºE, ~8 m depth), an area under governmental protection and considered a pristine site with no apparent human influence. Temperature (ºC), salinity (PSU), and DO data were obtained hourly by using SBE37-SMP-ODO (Sea-Bird Scientific Electronics®) and a MiniDot. Both sensors were attached to a mooring line at around 4 m depth. The manufacturer accuracy of measurements was ± 0.002ºC, 0.003 mS/cm, and ± 5% for temperature, conductivity, and oxygen sensors, respectively. Samples for dissolved nitrous oxide (N_2O), dissolved oxygen (DO), dissolved organic carbon (DOC), inorganic nutrients nitrate (NO_3^-), nitrite (NO_2^-), phosphate (PO_4^{3-}), silicate ($Si(OH)_4$), ammonia (NH_4) and Total Phosphorous (TP) and Total Nitrogen (TN) were collected monthly from the same depth as the sensors of the fixed stations.

The third sampling point is located in the coastal area near the Cape Ses Salines lighthouse (CS: 39.2649º N, 3.0535º E, Figure 1B). At this site, with a total bottom depth of 2 m, data were collected biweekly from surface water directly off the coast. Temperature (ºC), salinity (PSU), N_2O, DOC, and inorganic nutrients were obtained from the same volume of surface water. Oxygen data were obtained with a MiniDot sensor from August 2022. DO sensor data validation was performed with BP and CA stations DO water samples as described in Agueda-Aramburu et al. (2024).

2.2 Data collection and analysis

https://doi.org/10.5194/egusphere-2024-4166
Preprint. Discussion started: 23 January 2025

2.2.1 Biogeochemical variables

To determine Nitrous oxide (N_2O) levels, samples were collected in duplicate using 120 mL serum vials sealed with grey-butyl rubber stoppers and aluminium crimps. After being sealed, the samples were preserved with $HgCl_2$ and stored upside-down until analysis. N_2O concentrations were analyzed at the AQUANITROMET laboratory (https://www.iim.csic.es/en/about-iim/organization/aquanitromet-analysis-greenhouse-effect-gases-natural-waters) of the Instituto de Investigaciones Marinas (IIM-CSIC, Vigo, Spain) using a static headspace equilibration technique combined with gas chromatography (GC) equipped with electron capture detection, following the methodology detailed by De la Paz et al. (2015). To create the headspace, 20 mL of nitrogen gas from a Tedlar bag at atmospheric pressure was introduced into the vials, simultaneously extracting the same volume of water sample using a double-needle setup. The vials were shaken and left to equilibrate for at least 12 hours in a temperature-controlled environment. For injection into the GC, a brine solution was added through one needle to displace the headspace gas into the GC via the second needle.

The gas chromatograph, an Agilent 7890 GC, was calibrated using three standard gas mixtures: a NOAA-certified primary standard with a composition resembling atmospheric air, and two additional N_2O-in-N_2 mixtures supplied by Air Liquide (De la Paz et al., 2015). During participation in the first large-scale international Inter-Laboratory Comparison experiment for seawater N_2O measurements (Wilson et al., 2018), an additional certified standard from the Scientific Committee for Oceanographic Research (SCOR) was used. The precision of the analysis was determined to be 0.5%, calculated from the average coefficient of variation across 400 replicate measurements.

To determine the dissolved oxygen (DO) concentration, samples were analyzed following the Winkler method modified by Benson and Krause (1984) by potentiometric titration with a Metrohm 808 Titrando. The precision of the DO analysis was estimated to be lower than ± 2 µmol kg^{-1}.

Chl *a* samples were collected in glass bottles and filtered in the laboratory with a Whatman GF/F glass fiber filter. Chl *a* extraction was done with 90% acetone for 24 h in dark conditions, and samples were measured with a fluorometer (Turner Designs Instrument, Model 7200-00). The fluorometer was calibrated with a pure Chl *a* standard from *Anacystis nidulans* algae, Sigma Chemical Company (Knap et al., 1996).

DOC samples were filtered with pre-combusted Whatman GF/F glass fiber filters and stored in pre-combusted borosilicate vials fixed with 25 µL of orthophosphoric acid (H_3PO_4). Samples were analyzed by using a Shimadzu TOC-L analyzer following the analysis methodology described by Álvarez-Salgado and Miller (1998) based on catalytic oxidation at a high temperature (680 ºC).

Concentrations of NO_3^-, NO_2^-, PO_4^{3-}, Si $(OH)_4$, NH_4, and Total Nitrogen and Total Phosphorous were obtained from the analysis laboratory located at the Mediterranean Center for Marine and Environmental Research (CMIMA, Barcelona, Spain) with the Autoanalyser AA3 HR (Seal Analytical, United Kingdom) by continuous flow analysis. The precision estimated from the coefficient of variation based on replicate analysis of the same water samples (n = 10) ranged from 0.13 to 0.5 %.

2.2.2 Meteorological and atmospheric data

Wind speed at 10 m height was provided by the Agencia Estatal de Meteorología (AEMET) from the Sant Joan airport, Palma (Spain) station. Monthly averaged data of atmospheric N_2O molar fraction was obtained

https://doi.org/10.5194/egusphere-2024-4166
Preprint. Discussion started: 23 January 2025

from the monitoring station of Lampedusa (LMP), Italy, of the NOAA (National Oceanic and Atmospheric data Administration) monitoring network (http://www.esrl.noaa.gov/gmd/dv/site/;Lan et al. 2024)

2.3 Flux estimation and other calculations

To calculate the water-atmosphere N_2O fluxes (μmol m^{-2} d^{-1}) the following equation was used:

$$F = k * (Cw - C^*) \quad (1)$$

Where k (cm h^{-1}) is the gas transfer velocity, Cw is the concentration of N_2O dissolved in water samples (mol^{-1}), C^* is the gas saturation concentration that is calculated as the product between the atmospheric fraction of N_2O and the solubility coefficient proposed by (Weiss et al., 1980). To compute the fluxes of N_2O, we used the monthly mean of atmospheric molar N_2O obtained from NOAA.

The most appropriate parameterization for the gas transfer (k) in coastal areas with seagrass ecosystems characterized by a limited wind fetch, representing the study area in the Balearic Sea, was used. This equation was described by Dobashi and Ho (2023) as follows:

$$k = 0.143 \ U_{10}^2 \quad (2)$$

Emissions to the atmosphere are indicated by positive values.

Additionally, saturation values for N_2O (Sat%N_2O), expressed as a percentage, were computed as the ratio between the N_2O concentration observed and the calculated equilibrium concentration and ΔN_2O as the difference between N_2O observations and N_2O solubility concentration value. The Apparent Oxygen Utilization (AOU) was calculated using measured DO values and the solubility of oxygen gas in seawater (Benson and Krause, 1989).

2.4 Data Analysis

To test for differences in N_2O concentrations and fluxes between regions and on temporal scales, simple multifactorial general linear model analyses were implemented in MATLAB version 9.10.0 (R20211, MathWorks Inc.).

The influence of environmental drivers on N_2O levels was tested by the supervised Machine Learning (ML) Gradient Boosting Machine (GBM) based on decision tree models using a Cross-Validated Boosting (CVB). GBM is based on the specific implementation of an ensemble method that combines sequenced base weak models to create a stronger one by applying gradient descent to minimize the model loss function. In each iteration, a new model adjusts to the previous combined model residual in each iteration. The combination of all the base models is performed by summing their predictions, and to avoid overestimation, a weighted learning factor is applied. CVB technique allows a more precise evaluation of the model by using different datasheets to train and test the model repeatedly. GBM and CVB were implemented in Python version 3.12.3 using the XGBoost library (Chen and Guestrin, 2016).

The correlation between the response of N_2O and the resulting most dominant environmental variables (relative importance >10%) obtained from the CVB was analyzed through Ordinary Least Squares regression (OLS) of the Statsmodels library (Seabold and Perktold, 2010)in Python version 3.12.3. and by using Generalized Additive Models (GAM) with the pyGAM library (Servén and Brummitt, 2020) in Python version 3.12.3 to resolve the nonlinear dependency.

https://doi.org/10.5194/egusphere-2024-4166
Preprint. Discussion started: 23 January 2025

To determine the simple linear correlation between environmental variables on FN_2O, Pearson correlation coefficients and *p*-values were calculated for each station using the Scipy library (Virtanen et al., 2020) in Python version 3.12.3. Furthermore, a multiple linear regression analysis was performed to analyze the impact of numerous predictor variables on the FN_2O by applying an OLS.

3 Results and discussion

3.1 Environmental Variables Description

The observed seawater temperature patterns during the study period reflect the climatic characteristics of the Mediterranean region, with peak temperatures recorded in summer, notably reaching their maximum in August 2022, registering 30.3, 29.9, and 29°C in the BP, CA, and CS sites, respectively (Fig. 2A, Table 1). Conversely, minimum temperatures recorded during winter were 13.7°C in 2023 for BP, 13.04°C in 2023 for CA, and 13°C in 2019 for CS. Over the entire study period, average (± standard deviation) temperature values stood at 20.9 ± 5.1, 20.7 ± 4.9, and 20.4 ± 5.0°C for BP, CA, and CS, respectively, with no statistical differences between sites ($p > 0.05$, Table 1) but denoted variability between months and years ($p < 0.005$, Table 1).

Surface salinity levels exhibited significant differences between sites ($p < 0.005$ with CS values), months ($p < 0.005$), and years ($p < 0.05$), maintaining average values of 37.5±0.2 practical salinity units (psu) for BP, 37.4±0.2 psu for CA, and 37.7 ±0.3 psu for CS. The highest salinity levels were recorded during the summer of 2018 at BP (38.2 psu), the winter of 2023 at CA (38.0 psu), and both the summer of 2018 and winter of 2023 at CS (38.2 psu) (Fig. 2B, Table 1). The difference in the factory precision of the sensors that determine conductivity and, therefore, salinity could cause the differences between the CS and PB, and CA stations in salinity.

Wind speed measurements taken at a height of 10 meters exhibited an observable seasonal trend (Fig. 2C). However, no statistical differences were found between years and months ($p > 0.05$). Maximum averaged values appear during spring, balanced around 3.7 ± 0.4 ms^{-1}, and decline during winter to 2.9 ± 0.5 ms^{-1} over the study period. Maximum peak values were noted in December and January, reaching levels up to 19.9 ms^{-1}.

3.2 Nitrous oxide and related biogeochemical variables.

Over the monitored period from 2018 to 2023, dissolved N_2O concentrations displayed a seasonal pattern ($p < 0.005$, Table 1, Figure 3A), ranging from 6.5 to 9.9 nmol L^{-1}, with no significant disparities between stations and years ($p > 0.05$). The highest levels were recorded during the winter season, averaging 9.0 ± 0.2 nmol L^{-1} (with a peak in February), followed closely by autumn with 8.2 ± 0.6 nmol L^{-1} and spring with 7.9 ± 0.7 nmol L^{-1} (Table 1). Conversely, the lowest values were observed in summer, averaging 6.9 ±0.2 nmol L^{-1}, with the minimum recorded in August 2021 in PB. Opposite trends were observed in Sat%N_2O levels, with maximum values in summer and autumn and minimum in winter, ranging from 93 to 116.7% (Table 1).

Chl *a* followed a discernible seasonal pattern (Fig. 3B, Table 1), with significant disparities between sites, years, and months ($p < 0.005$). In January, we found the highest productivity with a mean Chl *a* value of

https://doi.org/10.5194/egusphere-2024-4166
Preprint. Discussion started: 23 January 2025

0.4 ± 0.2 µg L^{-1}, while May recorded the lowest at 0.2 ± 0.05 µg L^{-1}. PB exhibited the highest levels of 0.3 ± 0.2 µg L^{-1}, whereas CA (0.2 ± 0.2 µg L^{-1}) and CS (0.2 ± 0.1 µg L^{-1}) displayed similar concentrations. In 2019, all the stations exhibited the strongest Chl *a* signal (Fig. 3B)

DO presents monthly significant differences found for all the stations ($p < 0.005$, Table 1). During the spring season, DO levels reached their peak, up to 300 µmol kg^{-1}, while towards the end of the summer season, minimum values around 160 µmol kg^{-1} were recorded, particularly at the CA site. The average levels from 2018 to 2023 were coherent between BP and CA, with 233.5±22.0 and 231.8 ± 25.3 µmol kg^{-1}, respectively. In contrast, only limited sensor data were available for CS (Fig. 3D, green dots). However, it is well-known that the relevant oxygen production in the area is strongly related to the denoted presence of seagrass meadows, dominated by the endemic species *Posidonia oceanica,* as previously signaled in Aramburu et al. (2024) in the exact CA station location of this study.

AOU values were predominantly negative (Table 1), with averaged values of -14.1 ± 12.0, -11.9 ± 15.3, and -15.1 ± 4.9 µmol kg^{-1} for PB, CA and CS sites, respectively. AOU negative levels indicate the DO produced by the excess of photosynthesis versus respiration, which is well-fitted with the organic matter content observed from the DOC data (Fig. 3C). In the coastal Balearic Sea, DOC revealed similarities between sites and years ($p > 0.05$), with significant differences among months ($p < 0.05$). During the summer season, the highest average levels of 83.9 ± 0.9 µM were recorded, while winter exhibited the lowest of 73.8 ± 1.5 µM (Fig. 3F, Table 1). DOC data variability was notable in spring and autumn, with average values of 76.0 ± 5.9 and 76.6 ± 3.1 µM, respectively.

NO_3^- levels varied from 0.1 to 6.3 during the study period, with no significant differences between months but differences between years ($p < 0.005$) and sites ($p < 0.005$), with CS showing the highest NO_3^- levels with average values of 1.5 ± 1.5 µM, followed by PB with 0.3 ± 0.4 µM and CA the lowest with 0.1 ± 0.2 µM (Fig. 3E, Table 1). NO_2^- concentrations were significantly different between years ($p < 0.005$; Fig. 3F, Table 1) and between stations ($p < 0.05$ for CA, Table 1), with total averaged values of 0.03 ± 0.02, 0.05 ± 0.05 and 0.07 ± 0.06 µM for CA, PB and CS, respectively.

The analysis of the effect of environmental and biogeochemical variables on the N_2O concentrations through the CVB resulted in only seven main parameters associated with the N_2O variability (Fig. 4). These were, in order of importance: temperature (65 %), Chl *a* (17 %), salinity (7%), dissolved organic carbon (5 %), nitrate (4 %) and nitrite (2 %).

Temperature values, the first variable modeling the N_2O concentrations, presented a strong decreasing linear correlation with N_2O levels with $p<0.005$ and an R^2 of 0.94 for all the stations evaluated (not shown). The N_2O solubility decreases in warmer waters, explaining the observed maximum and minimum seasonal pattern of N_2O, which is primarily governed by the thermodynamic influence of temperature on N_2O concentrations. The Sat%N_2O used here as a proxy of the biological consumption/production of N_2O shows a positive linear correlation with temperature ($p<0.005$ and an R^2 of 0.59; Fig. 5). This positive correlation is expected since the microbial activity of nitrification and denitrification is assumed to rise with increasing temperatures, followed by N_2O production (Wu et al., 2018). However, our results indicate that the control of seasonality of N_2O by thermodynamic solubility exceeded the promotion of microbial activity.

The DO availability and the predominance of negative AOU levels with no correlation with Sat%N_2O ($p>0.05$, $R^2=0.002$) suggest that *in situ* N_2O production has a minor contribution to the observed temporal

https://doi.org/10.5194/egusphere-2024-4166
Preprint. Discussion started: 23 January 2025

N_2O variability. Overall, the low importance of predictors of the CVB analysis, such as Chla, DO, DOC, nitrate and nitrite, is consistent with low N_2O production from nitrification, associated with the remineralization seasonal cycle of organic matter, which is enhanced in the high-productivity conditions. Microbial production by nitrification and denitrification are generally considered the dominant pathways of N_2O biological production in the shelf sea and open ocean (Burgos et al., 2017; Chen et al., 2021; de la Paz et al., 2024; Sierra et al., 2020). However, in the oxygenated coastal Balearic Sea waters, the near-equilibrium values for Sat%N_2O and low NO_3^- and NO_2^- values (Figs. 3E-F, 5, Table 1) point to a minor contribution of the pelagic nitrification.

In addition, the CBV analysis points to Chl *a* as the second driver explaining the observed N_2O variability since the observed seasonal cycle of Chl *a* is coupled to the N_2O, with maximum values in winter and minimum in summer. A hypothetic mechanism that could be contributing to the N_2O variability in our study site is the poorly described production of N_2O by epipelagic photosynthetic organisms in the light through NO reduction (Burlacot et al., 2020).

Finally, unexpected significant negative ($p<0.05$) linear correlations were found between N_2O levels and silicate only at PB and CA sites (Table 1) with -0.41 and -0.34 correlation coefficients, respectively. This relation and the obtained differences in salinity values between PB and CA to CS can denote the presence or absence of groundwater input pulses in these areas (Basterretxea et al., 2010; Sospedra et al., 2018) that can affect N_2O concentrations in specific coastal regions (Calvo-Martin et al., 2024). As this relation was only observed in two of the three stations considered, this parameter was not included in the CVB analysis.

An OLS regression was performed to evaluate the relation of the three variables with the higher relative importance for N_2O concentrations (Importance >5%), representing 89% of the variability (Temperature, Chl *a* and salinity, Fig. 4) obtained in the CVB analysis. The equation obtained was: $N_2O = 7.42 - 0.18 * \text{Temperature} + 0.28 * \text{Chl } a + 0.11 * \text{Salinity}$ ($R^2 = 0.94$) with a p-value<0.005 for temperature and a p-value of 0.07 for Chl *a* and 0.152 for salinity.

To resolve the nonlinear dependency of the Chl *a* and salinity with N_2O concentrations, a GAM was applied, explaining 96 % of the response variable with a p-value <0.005 for temperature and <0.05 for Chl *a* and 0.1390 for salinity (Supplemented figures). The non-significance for salinity could be because GAM smooth terms are designed to capture broader nonlinear effects. In this case, Salinity might either not have a robust and smooth effect or its impact is masked by other variables like temperature. The GAM residuals ranged from -0.6 to 0.6 nmol L^{-1} (Supplemented figures).

Placing the obtained data in a global ocean context, concretely among studied coastal areas, the Balearic Sea presents similar levels to the range found in 2008 in the Bohai Sea between 7.14-8.32 nmol L^{-1} (Gu et al., 2022), but small when compared to upwelling and estuarine coastal areas. Maximum N_2O levels found in this study represent approximately baseline levels for the rest of the coastal and open ocean areas evaluated previously (Bange, 2006; Bange et al., 1996; de la Paz et al., 2024; Yang et al., 2009; Zhang et al., 2008).

3.3 Air-sea N_2O exchange

FN_2O values ranged from -0.3 to 0.6 µmol m^{-2} d^{-1} over the study period, acting the coastal Balearic Sea area as a minor sink or nearly in equilibrium in winter and spring and as a light source in summer and

https://doi.org/10.5194/egusphere-2024-4166
Preprint. Discussion started: 23 January 2025

autumn (Fig. 6; $p < 0.005$) following the seasonality of temperature (Fig. 6, grey line) closely. No differences between years were observed. However, significant differences were noted between sites, with PB exhibiting the highest FN_2O and CA the lowest ($p < 0.05$).

In the PB site, positive linear correlations were found between FN_2O with temperature (r = 0.67; $p < 0.005$) and with ΔN_2O (r = 0.96; $p < 0.005$). In the OLS analysis, wind speed appears to exert also a positive influence on FN_2O values, only detectable in PB data (OLS, $R^2 = 0.94$, $p < 0.05$), likely attributable to its geographical characteristics, as PB represents an open bay in contrast to the enclosed CA station in Santa Maria Bay sampling site and the shallow coastal waters of CS.

FN_2O in the most pristine station CA showed positive correlations also with temperature (r = 0.79; $p < 0.005$), ΔN_2O (r = 0.97; $p < 0.005$) and the Sat%N_2O (r = 0.97; $p < 0.005$).

CS shallow site presented positive lineal correlations along temperature (r = 0.73; $p < 0.005$), with ΔN_2O (r = 0.98; $p < 0.005$) and the Sat%N_2O (r = 0.97; $p < 0.005$). Salinity was also a predicting variable presented in the OLS analysis (OLS, $R^2 = 0.96$, $p < 0.05$) negatively related. This characteristic can be related to the differences in CS salinity values with the other stations.

Annual average fluxes for the three sites were calculated, and when monthly data was unavailable, a linear interpolation was applied (Table 2). The results showed that all the stations are minor sources of N_2O to the atmosphere, with notably higher values in the PB station, as observed in the daily FN_2O values (Fig. 6). PB presented an apparent interannual variability during the study period (Table 2). The CS and CA sites followed the same trend as the PB station but with significantly lower values, especially for CA. Observed annual N_2O fluxes in the Balearic Sea are considerably lower than the expected ranges for this ocean region, as described by Resplandy et al. (2024) based on global reconstruction products from 1985 to 2018 (Yang et al., 2020). These differences could relate to the large variability in local N_2O fluxes in coastal areas with vegetation. Coastal regions with seagrass meadows are expected to have the lowest N_2O flux ranges (Rosentreter et al., 2023). These areas are considered negligible sources (Al-Haj et al., 2021) or sinks in near-pristine seagrasses, resulting in strongly biased coastal global estimations (Chen et al., 2022).

Considering that European seagrasses constitute 6% of the global seagrass meadows and that most of this coverage is allocated in the Mediterranean Sea, it is imperative to know more about the drivers of the formation and consumption seasonality and the transport pathways. Also, the increase in the number of observations is critical because nitrous oxide data in the Mediterranean Sea is scarce. In addition, we have to take into account the ongoing coastal eutrophication related to anthropogenic inputs from estuaries, sewage sites from highly populated coastal areas, and industrial effluents that may well significantly modify seagrass habitats as well as current emissions of N_2O from coastal zones (Bakker et al., 2014).

As coastal N_2O emissions are assumed to offset 30-58% of net CO_2 coastal uptake radiative effect (Resplandy et al., 2024), estimating the water N_2O emission-based Global Warming Potential (GWP) can give us a clear picture by comparing with existing data on CO_2 and methane fluxes in the area. By following the Intergovernmental Panel on Climate Change (IPCC) Assessment Report 6 (Arias et al., 2021) updated 100-year GWP, we obtained the GWP_{N2O} (i.e., the 100-year time-integrated radiative forcing from the instant release of 1 kg of N_2O is 273 times larger than the forcing of 1 kg of CO_2). In the coastal Balearic Sea, considering an area of 1km distance offshore and 1428 km of coastal longitude, the average GWP_{N2O} obtained in this study is $8.1*10^{-7} \pm 5.7*10^{-7}$ Pg CO_2-eq y^{-1} for all the sites from 2020 to 2022, which was

https://doi.org/10.5194/egusphere-2024-4166
Preprint. Discussion started: 23 January 2025

the period with more available data. Comparing with the annual GWP_{CO2} of $2.3\pm*10^{-6} \pm 4.6*10^{-5}$ g CO_2 y^{-1} obtained in the coastal Balearic Sea from the available data from Flecha et al. (2023), we can confirm that N_2O emissions in this area are not substantial yet in terms of GWP regarding other GHGs. However, the offset of 35% obtained in this study for N_2O closely follows the assumption by Resplandy et al. (2024).

4 Conclusions

N_2O concentrations in seawater during the study period ranged from 6.5 to 9.9 nM without significant differences between the three sampling sites. Several drivers dominated the N_2O variability, with temperature as the most essential factor and less critical Chlorophyll *a* and salinity. Even with the possible biological implications in N_2O formation, atmospheric forcing may control the surface concentrations in this area. Averaged estimated N_2O fluxes oscillated between -0.3 and 0.6 µmol m^{-2} $d^{-1,}$ with the most impacted stations showing the highest N_2O fluxes. All areas generally behaved as weak N_2O sources, following a robust seasonal pattern throughout the sampling period. Reducing anthropogenic pressures in coastal regions is crucial to preserving marine ecosystems, as increasing human impacts, such as pollution, overfishing, and habitat destruction, can lead to irreversible damage, loss of biodiversity, and the degradation of vital ecosystem services. If these pressures continue to escalate, future projections indicate more frequent and severe environmental crises, including increased coastal erosion, declining fish stocks, and heightened vulnerability to climate change, threatening marine life and human coastal communities. There is a strong need to increase the number of observations of the Greenhouse Gas nitrous oxide in coastal areas to understand the dominating drivers to elaborate more exact predictions of future consequences under additional anthropogenic impacts. In addition, the presented values for the coastal Balearic Sea will contribute to an improved estimation of global N_2O emissions budgets in coastal vegetated areas in general.

Data availability

Data was obtained from the Metocean Data Repository of the Balearic Islands Coastal Observing and Forecasting System (SOCIB). 2024, Data from the instruments on the Palma Bay Station platform, https://apps.socib.es/data-catalog, data consulted on 01-30-2024. Data is also accessible through Tintoré & Casas (2022) and Hendriks et al. (2023).

Supplement link

Author contribution

IE, JT, and SF conceptualized the research, data acquisition approach, and methodology; IE, SF, MdP, CM and AEF collected the samples and performed the measurements; SF, MdP and IE analyzed the data; SF wrote the manuscript draft; All authors reviewed and edited the manuscript.

Competing interests

The authors declare no competing financial interest.

Acknowledgments

https://doi.org/10.5194/egusphere-2024-4166
Preprint. Discussion started: 23 January 2025

We are grateful to the Cabrera National Park staff for facilitating the work performed during this study and to the Balearic Islands Coastal Observing and Forecasting System (SOCIB) for their invaluable help and use of their fixed station in the Bay of Palma. We thank Lidia Cucala (IMEDEA), Andrea Carbonero and Juan Martínez Ayala (SOCIB) for their assistance with sample collection and analysis. This work is a contribution to CSIC Thematic Interdisciplinary Platform PTI OCEANS+. We thank the AQUANITROMET service of Instituto Investigaciones Marinas for the methane analyses and the Agencia Estatal de Meteorología (AEMET) for providing the meteorological data.

Financial support

Funding for this work was provided by the Spanish Ministry of Science (SumaEco, RTI2018–095441-B-C21, CYCLE, PID2021-123723OB-C21), the Government of the Balearic Islands through la Consellería d'Innovació, Recerca i Turisme (Projecte de recerca científica i tecnològica SEPPO, PRD2018/18) and the 2018 call of BBVA Foundation "Ayudas a equipos de investigación científica" as the Posi-COIN Project. SF acknowledges the financial support of "Margalida Comas-2017" and "Vicenç Munt Estabilitat-2022" postdoctoral contracts and project AAEE111/2017 from the Balearic Islands Government and the MMT24-PTI+OCEANS-01 postdoctoral contract funded by the European Union NextGenerationEU. MP acknowledges the financial support during the study period to the contracts financed by the Spanish Ministry of Science CTM2015–74510-JIN and PTA2019–017983-I.

References

Agueda Aramburu, P., Flecha, S., Lujan-Williams, C. A. M., and Hendriks, I. E.: Water column oxygenation by Posidonia oceanica seagrass meadows in coastal areas: A modelling approach, Science of the Total Environment, 942, 173805, https://doi.org/10.1016/j.scitotenv.2024.173805, 2024.

Al-Haj, A. N., Chidsey, T., Fulweiler, R. W., Rosentreter, J. A., Al-Haj, A. N., Fulweiler, R. W., Williamson, P., Laruelle, G. G., Bange, H. W., Bianchi, T. S., Busecke, J. J. M., Cai, W. J., Eyre, B. D., Forbrich, I., Kwon, E. Y., Maavara, T., Moosdorf, N., Najjar, R. G., Sarma, V. V. S. S., Van Dam, B., and Regnier, P.: Two temperate seagrass meadows are negligible sources of methane and nitrous oxide, Nat Clim Chang, 35, 579–587, https://doi.org/10.1002/lno.12250, 2021.

Álvarez-Salgado, X. A. and Miller, A. E. J.: Simultaneous determination of dissolved organic carbon and total dissolved nitrogen in seawater by high temperature catalytic oxidation: Conditions for precise shipboard measurements, Mar Chem, 62, 325–333, https://doi.org/10.1016/S0304-4203(98)00037-1, 1998.

Arias, P., Bellouin, N., Coppola, E., Jones, R., Krinner, G., Marotzke, J., Naik, V., Palmer, M., Plattner, G.-K., and Rogelj, J.: Climate Change 2021: The Physical Science Basis. Contribution of Working Group14 I to the Sixth Assessment Report of the Intergovernmental Panel on Climate Change; Technical Summary, 2021.

Bakker, D. C. E., Bange, H. W., Gruber, N., Johannessen, T., Upstill-Goddard, R. C., Borges, A. V., Delille, B., Löscher, C. R., Naqvi, S. W. A., Omar, A. M., and Magdalena Santana-Casiano, J.: Air-sea interactions of natural long-lived greenhouse gases (CO_2, N_2O, CH_4) in a changing climate, in: Ocean-Atmosphere Interactions of Gases and Particles, Springer Berlin Heidelberg, 113–169, https://doi.org/10.1007/978-3-642-25643-1_3, 2014.

Bange, H. W.: Nitrous oxide and methane in European coastal waters, Estuar Coast Shelf Sci, 70, 361–374, https://doi.org/10.1016/j.ecss.2006.05.042, 2006.

Bange, H. W., Rapsomanikis, S., and Andreae, M. O.: Nitrous oxide in coastal waters, Global Biogeochemical Cycles, German, 132 pp., 1996.

Barbier, E. B., Hacker, S. D., Kennedy, C., Koch, E. W., Stier, A. C., and Silliman, B. R.: The value of estuarine and coastal ecosystem services, Ecol Monogr, 81, 169–193, https://doi.org/https://doi.org/10.1890/10-1510.1, 2011.

Basterretxea, G., Tovar-Sanchez, A., Beck, A. J., Masqué, P., Bokuniewicz, H. J., Coffey, R., Duarte, C. M., Garcia-Orellana, J., Garcia-Solsona, E., Martinez-Ribes, L., and Vaquer-Sunyer, R.: Submarine groundwater discharge to the coastal environment of a Mediterranean island (Majorca, Spain): Ecosystem and biogeochemical significance, Ecosystems, 13, 629–643, https://doi.org/10.1007/s10021-010-9334-5, 2010.

Benson, B. B. and Krause, D.: A thermodynamic treatment of dilute solutions of gases in liquids, J Solution Chem, 18, 803–821, https://doi.org/10.1007/BF00685061, 1989.

Benson, B. B. and Krause Jr., D.: The concentration and isotopic fractionation of oxygen dissolved in freshwater and seawater in equilibrium with the atmosphere, Limnol Oceanogr, 29, 620–632, https://doi.org/https://doi.org/10.4319/lo.1984.29.3.0620, 1984.

Bianchi, C. N. and Morri, C.: Marine biodiversity of the Mediterranean Sea: Situation, problems and prospects for future research, Mar Pollut Bull, 40, 367–376, https://doi.org/10.1016/S0025-326X(00)00027-8, 2000.

Burgos, M., Ortega, T., and Forja, J. M.: Temporal and spatial variation of N_2O production from estuarine and marine shallow systems of Cadiz Bay (SW, Spain), Science of the Total Environment, 607–608, https://doi.org/10.1016/j.scitotenv.2017.07.021, 2017.

Burlacot, A., Richaud, P., Gosset, A., Li-Beisson, Y., and Peltier, G.: Algal photosynthesis converts nitric oxide into nitrous oxide, PNAS, 117, 2704–2709, https://doi.org/10.1073/pnas.1915276117/-/DCSupplemental, 2020.

Calvo-Martin, E., de la Paz, M., Álvarez-Salgado, X. A., Pazó Fernández, M. J., Vieitez Dos Santos, V., and Ibánhez, J. S. P.: Transport and reactivity of nitrous oxide and methane in two contrasting subterranean estuaries, Limnol Oceanogr, 1–16, https://doi.org/10.1002/lno.12622, 2024.

Carstensen, J. and Duarte, C. M.: Drivers of pH Variability in Coastal Ecosystems, Environ Sci Technol, 53, 4020–4029, https://doi.org/10.1021/acs.est.8b03655, 2019.

Chen, T. and Guestrin, C.: XGBoost: A Scalable Tree Boosting System, in: Proceedings of the 22nd ACM SIGKDD International Conference on Knowledge Discovery and Data Mining, 785–794, https://doi.org/10.1145/2939672.2939785, 2016.

Chen, X., Ma, X., Gu, X., Liu, S., Song, G., Jin, H., and Zhang, G.: Seasonal and spatial variations of N_2O distribution and emission in the East China Sea and South Yellow Sea, Science of the Total Environment, 775, 145715, https://doi.org/10.1016/j.scitotenv.2021.145715, 2021.

Codispoti, L. A.: Interesting Times for Marine N_2O, Science (1979), 327, 1339–1340, https://doi.org/10.1126/science.1184945, 2010.

Dobashi, R. and Ho, D. T.: Air–sea gas exchange in a seagrass ecosystem–results from a ^{3}He/SF^6 tracer release experiment, Biogeosciences, 20, 1075–1087, 2023.

Doney, S. C.: The growing human footprint on coastal and open-ocean biogeochemistry, Science (1979), 328, 1512, 2010.

Duarte, C. M., Middelburg, J. J., and Caraco, N.: Major role of marine vegetation on the oceanic carbon cycle, Biogeosciences, 2, 1–8, https://doi.org/10.5194/bg-2-1-2005, 2005.

EEA: State and pressures of the marine and coastal Mediterranean environment, European Environment Agency, 1–44, 1999.

Farías, L., Paulmier, A., and Gallegos, M.: Nitrous oxide and N-nutrient cycling in the oxygen minimum zone off northern Chile, Deep Sea Research Part I: Oceanographic Research Papers, 54, 164–180, https://doi.org/https://doi.org/10.1016/j.dsr.2006.11.003, 2007.

Flecha, S., Giménez-Romero, À., Tintoré, J., Pérez, F. F., Alou-Font, E., Matías, M. A., and Hendriks, I. E.: pH trends and seasonal cycle in the coastal Balearic Sea reconstructed through machine learning, Sci Rep, 12, 12956, https://doi.org/10.1038/s41598-022-17253-5, 2022.

Flecha, S., Rueda, D., de la Paz, M., Pérez, F. F., Alou-Font, E., Tintoré, J., and Hendriks, I. E.: Spatial and temporal variation of methane emissions in the coastal Balearic Sea, Western Mediterranean, Science of the Total Environment, 865, https://doi.org/10.1016/j.scitotenv.2022.161249, 2023.

Giorgi, F.: Climate change hot-spots, Geophys Res Lett, 33, https://doi.org/https://doi.org/10.1029/2006GL025734, 2006.

Giorgi, F. and Lionello, P.: Climate change projections for the Mediterranean region, Glob Planet Change, 63, 90–104, https://doi.org/10.1016/j.gloplacha.2007.09.005, 2008.

Gu, T., Jia, D., Wang, Z., Guo, Y., Xin, Y., Guo, C., Zhang, G., and Sun, J.: Regional distribution and environmental regulation mechanism of nitrous oxide in the Bohai Sea and North Yellow Sea: A preliminary study, Science of the Total Environment, 818, https://doi.org/10.1016/j.scitotenv.2021.151718, 2022.

Hendriks, I. E., Escolano-Moltó, A., Flecha, S., Vaquer-Sunyer, R., Wesselmann, M., and Marbà, N.: Mediterranean seagrasses as carbon sinks: methodological and regional differences, Biogeosciences, 19, 4619–4637, https://doi.org/10.5194/bg-19-4619-2022, 2022.

Hendriks, I. E., Flecha, S., de La Paz, M., Pérez, F. F., Morell, C., Tintoré, J., and Marbà, N.: Methane emissions in the coastal Balearic Sea between October 2019 - October 2021, DIGITAL CISC, https://doi.org/10.20350/digitalCSIC/15491, 2023.

Knap, A., Michaels, A., Close, A., Ducklow, H., and Dickson, A.: Protocols for the Joint Global Ocean Flux Study (JGFOS) Core Measurements, JGOFS Reoprt Nr. 19, vi+170 pp, 198, 1996.

de la Paz, M., Huertas, I. E., Flecha, S., Ríos, A. F., and Pérez, F. F.: Nitrous oxide and methane in Atlantic and Mediterranean waters in the Strait of Gibraltar: Air-sea fluxes and inter-basin exchange, Prog Oceanogr, 138, 18–31, https://doi.org/10.1016/j.pocean.2015.09.009, 2015a.

de la Paz, M., Huertas, I. E., Flecha, S., Ríos, A. F., and Pérez, F. F.: Nitrous oxide and methane in Atlantic and Mediterranean waters in the Strait of Gibraltar: Air-sea fluxes and inter-basin exchange, Prog Oceanogr, 138, 18–31, https://doi.org/10.1016/j.pocean.2015.09.009, 2015b.

https://doi.org/10.5194/egusphere-2024-4166
Preprint. Discussion started: 23 January 2025

de la Paz, M., Pérez, F. F., Álvarez, M., and Bode, A.: Seasonal ventilation controls nitrous oxide emission in the NW Iberian upwelling, Prog Oceanogr, 224, https://doi.org/10.1016/j.pocean.2024.103261, 2024.

Lan, X., Mund, J. W., Crotwell, A. M., Thoning, K. W., Moglia, E., Madronich, M., Baugh, K., Petron, G., Crotwell, M. J., Neff, D., Wolter, S., Mefford, T., and DeVogel, S.: Atmospheric Nitrous Oxide Dry Air Mole Fractions from the NOAA GML Carbon Cycle Cooperative Global Air Sampling Network, 1997-2023, https://doi.org/10.15138/53g1-x417, 2024.

Ma, X., Lennartz, S. T., and Bange, H. W.: A multi-year observation of nitrous oxide at the Boknis Eck Time Series Station in the Eckernförde Bay (southwestern Baltic Sea), Biogeosciences, 16, 4097–4111, https://doi.org/10.5194/bg-16-4097-2019, 2019.

Masson-Delmotte, V., Zhai, P., Pirani, A., Connors, S. L., Péan, C., Berger, S., Caud, N., Chen, Y., Goldfarb, L., Gomis, M. I., Huang, M., Leitzell, K., Lonnoy, E., Matthews, J. B. R., Maycock, T. K., Waterfield, T., Yelekçi, O., Yu, R., and Zhou, B.: Climate Change 2021: The Physical Science Basis. Contribution of Working Group I to the Sixth Assessment Report of the Intergovernmental Panel on Climate Change, in: Sixth Assessment Report of the Intergovernmental Panel on Climate Change, Cambridge University Press, 2021.

Micheli, F., Halpern, B. S., Walbridge, S., Ciriaco, S., Ferretti, F., Fraschetti, S., Lewison, R., Nykjaer, L., and Rosenberg, A. A.: Cumulative human impacts on Mediterranean and Black Sea marine ecosystems: assessing current pressures and opportunities, PLoS One, 8, e79889, 2013.

Mouillot, D., Albouy, C., Guilhaumon, F., Ben Rais Lasram, F., Coll, M., Devictor, V., Meynard, C. N., Pauly, D., Tomasini, J. A., Troussellier, M., Velez, L., Watson, R., Douzery, E. J. P., and Mouquet, N.: Protected and threatened components of fish biodiversity in the mediterranean sea, Current Biology, 21, 1044–1050, https://doi.org/10.1016/j.cub.2011.05.005, 2011.

Nevison, C. D., Weiss, R. F., and Erickson III, D. J.: Global oceanic emissions of nitrous oxide, J Geophys Res Oceans, 100, 15809–15820, https://doi.org/https://doi.org/10.1029/95JC00684, 1995.

Resplandy, L., Hogikyan, A., Müller, J. D., Najjar, R. G., Bange, H. W., Bianchi, D., Weber, T., Cai, W.-J., Doney, S. C., Fennel, K., Gehlen, M., Hauck, J., Lacroix, F., Landschützer, P., Le Quéré, C., Roobaert, A., Schwinger, J., Berthet, S., Bopp, L., Chau, T. T. T., Dai, M., Gruber, N., Ilyina, T., Kock, A., Manizza, M., Lachkar, Z., Laruelle, G. G., Liao, E., Lima, I. D., Nissen, C., Rödenbeck, C., Séférian, R., Toyama, K., Tsujino, H., and Regnier, P.: A Synthesis of Global Coastal Ocean Greenhouse Gas Fluxes, Global Biogeochem Cycles, 38, e2023GB007803, https://doi.org/https://doi.org/10.1029/2023GB007803, 2024.

Rosentreter, J. A., Laruelle, G. G., Bange, H. W., Bianchi, T. S., Busecke, J. J. M., Cai, W. J., Eyre, B. D., Forbrich, I., Kwon, E. Y., Maavara, T., Moosdorf, N., Najjar, R. G., Sarma, V. V. S. S., Van Dam, B., and Regnier, P.: Coastal vegetation and estuaries are collectively a greenhouse gas sink, Nat Clim Chang, 13, 579–587, https://doi.org/10.1038/s41558-023-01682-9, 2023.

Seabold, S. and Perktold, J.: statsmodels: Econometric and statistical modeling with python, in: 9th Python in Science Conference, 2010.

Servén, D. and Brummitt, C.: pyGAM Documentation, 2020.

Sierra, A., Jiménez-López, D., Ortega, T., Ponce, R., Bellanco, M. J., Sánchez-Leal, R., Gómez-Parra, A., and Forja, J.: Distribution of N_2O in the eastern shelf of the Gulf of Cadiz (SW Iberian Peninsula), Science of the Total Environment, 593–594, https://doi.org/10.1016/j.scitotenv.2017.03.189, 2017.

Sierra, A., Jiménez-López, D., Ortega, T., Gómez-Parra, A., and Forja, J.: Factors controlling the variability and emissions of greenhouse gases (CO_2, CH_4 and N_2O) in three estuaries of the Southern Iberian Atlantic Basin during July 2017, Mar Chem, 226, https://doi.org/10.1016/j.marchem.2020.103867, 2020.

Solomon, S., Qin, D., Manning, M., Averyt, K., and Marquis, M.: Climate change 2007-the physical science basis: Working group I contribution to the fourth assessment report of the IPCC, Cambridge University Press, Cambridge, United Kingdom and New York, NY, USA., 2007.

Sospedra, J., Niencheski, L. F. H., Falco, S., Andrade, C. F. F., Attisano, K. K., and Rodilla, M.: Identifying the main sources of silicate in coastal waters of the Southern Gulf of Valencia (Western Mediterranean Sea), Oceanologia, 60, 52–64, https://doi.org/10.1016/j.oceano.2017.07.004, 2018.

Tian, H., Pan, N., Thompson, R. L., Canadell, J. G., Suntharalingam, P., Regnier, P., Davidson, E. A., Prather, M., Ciais, P., Muntean, M., Pan, S., Winiwarter, W., Zaehle, S., Zhou, F., Jackson, R. B., Bange, H. W., Berthet, S., Bian, Z., Bianchi, D., Bouwman, A. F., Buitenhuis, E. T., Dutton, G., Hu, M., Ito, A., Jain, A. K., Jeltsch-Thömmes, A., Joos, F., Kou-Giesbrecht, S., Krummel, P. B., Lan, X., Landolfi, A., Lauerwald, R., Li, Y., Lu, C., Maavara, T., Manizza, M., Millet, D. B., Mühle, J., Patra, P. K., Peters, G. P., Qin, X., Raymond, P., Resplandy, L., Rosentreter, J. A., Shi, H., Sun, Q., Tonina, D., Tubiello, F. N., van der Werf, G. R., Vuichard, N., Wang, J., Wells, K. C., Western, L. M., Wilson, C., Yang, J., Yao, Y., You, Y., and Zhu, Q.: Global nitrous oxide budget (1980--2020), Earth Syst Sci Data, 16, 2543–2604, https://doi.org/10.5194/essd-16-2543-2024, 2024.

Tintoré, J. and Casas-Pérez, B.: Buoy Bahía de Palma Physicochemical parameters of sea water data (Version x.y.z), Balearic Islands Coastal Observing and Forecasting System, SOCIB, https://doi.org/10.25704/S6JB-CK61, 2022.

Tintoré, J., Vizoso, G., Casas, B., Heslop, E., Pascual, A., Orfila, A., Ruiz, S., Martínez-Ledesma, M. M., Torner, M., Cusí, S., Diedrich, A., Balaguer, P., Gómez-Pujol, L., Álvarez-Ellacuria, A., Gómara, S., Sebastian, K., Lora, S., Beltrán, J. P., Renault, L., Juzà, M., Álvarez, D., March, D., Garau, B. B., Castilla, C., Cañellas, T., Roque, D., Lizarán, I., Pitarch, S., Carrasco, M. A., Lana, A. A., Mason, E., Escudier, R., Conti, D., Sayol, J. M., Barceló, B., Alemany, F. F., Reglero, P., Massuti, E., Vélez-Belchí, P., Ruiz, J., Oguz, T., Gómez, M., Álvarez, E., Ansorena, L. L., Manriquez, M., Barceló-Llull, B., Alemany, F. F., Reglero, P., Massutí, E., Vélez-Belchí, P., Ruiz Segura, J., Oguz, T., Gómez, M., Álvarez-Fanjul, E., Ansorena, L. L., and Manríquez, M.: SOCIB: The Balearic Islands Coastal Ocean Observing and Forecasting System Responding to Science, Technology and Society Needs, Mar Technol Soc J, 47, 101–117, https://doi.org/10.4031/MTSJ.47.1.10, 2013.

Tintoré, J., Pinardi, N., Álvarez-Fanjul, E., Aguiar, E., Álvarez-Berastegui, D., Bajo, M., Balbin, R., Bozzano, R., Nardelli, B. B., Cardin, V., Casas, B., Charcos-Llorens, M., Chiggiato, J., Clementi, E., Coppini, G., Coppola, L., Cossarini, G., Deidun, A., Deudero, S., D'Ortenzio, F., Drago, A., Drudi, M., El Serafy, G., Escudier, R., Farcy, P., Federico, I., Fernández, J. G., Ferrarin, C., Fossi, C., Frangoulis, C., Galgani, F., Gana, S., García Lafuente, J., Sotillo, M. G., Garreau, P., Gertman, I., Gómez-Pujol, L., Grandi, A., Hayes, D., Hernández-Lasheras, J., Herut, B., Heslop, E., Hilmi, K., Juza, M., Kallos, G., Korres, G., Lecci, R., Lazzari, P., Lorente, P., Liubartseva, S., Louanchi, F., Malacic, V., Mannarini, G., March, D., Marullo, S., Mauri, E., Meszaros, L., Mourre, B., Mortier, L., Muñoz-Mas, C., Novellino, A., Obaton, D., Orfila, A., Pascual, A., Pensieri, S., Pérez Gómez, B., Pérez Rubio, S., Perivoliotis, L., Petihakis, G., de la

https://doi.org/10.5194/egusphere-2024-4166
Preprint. Discussion started: 23 January 2025

Villéon, L. P., Pistoia, J., Poulain, P. M., Pouliquen, S., Prieto, L., Raimbault, P., Reglero, P., Reyes, E., Rotllan, P., Ruiz, S., Ruiz, J., Ruiz, I., Ruiz-Orejón, L. F., Salihoglu, B., Salon, S., Sammartino, S., Sánchez Arcilla, A., Sannino, G., Sannino, G., Santoleri, R., Sardá, R., Schroeder, K., Simoncelli, S., Sofianos, S., Sylaios, G., Tanhua, T., Teruzzi, A., Testor, P., Tezcan, D., Torner, M., et al.: Challenges for Sustained Observing and Forecasting Systems in the Mediterranean Sea, Front Mar Sci, 6, https://doi.org/10.3389/fmars.2019.00568, 2019.

del Valle Villalonga, L., Pons, G. X., and Bardolet, M.: Posidonia oceanica Cartography and Evolution of the Balearic Sea (Western Mediterranean), Remote Sens (Basel), 15, https://doi.org/10.3390/rs15245748, 2023.

Virtanen, P., Gommers, R., Oliphant, T. E., Haberland, M., Reddy, T., Cournapeau, D., Burovski, E., Peterson, P., Weckesser, W., Bright, J., van der Walt, S. J., Brett, M., Wilson, J., Millman, K. J., Mayorov, N., Nelson, A. R. J., Jones, E., Kern, R., Larson, E., Carey, C. J., Polat, İ., Feng, Y., Moore, E. W., VanderPlas, J., Laxalde, D., Perktold, J., Cimrman, R., Henriksen, I., Quintero, E. A., Harris, C. R., Archibald, A. M., Ribeiro, A. H., Pedregosa, F., van Mulbregt, P., Vijaykumar, A., Bardelli, A. Pietro, Rothberg, A., Hilboll, A., Kloeckner, A., Scopatz, A., Lee, A., Rokem, A., Woods, C. N., Fulton, C., Masson, C., Häggström, C., Fitzgerald, C., Nicholson, D. A., Hagen, D. R., Pasechnik, D. V., Olivetti, E., Martin, E., Wieser, E., Silva, F., Lenders, F., Wilhelm, F., Young, G., Price, G. A., Ingold, G. L., Allen, G. E., Lee, G. R., Audren, H., Probst, I., Dietrich, J. P., Silterra, J., Webber, J. T., Slavič, J., Nothman, J., Buchner, J., Kulick, J., Schönberger, J. L., de Miranda Cardoso, J. V., Reimer, J., Harrington, J., Rodríguez, J. L. C., Nunez-Iglesias, J., Kuczynski, J., Tritz, K., Thoma, M., Newville, M., Kümmerer, M., Bolingbroke, M., Tartre, M., Pak, M., Smith, N. J., Nowaczyk, N., Shebanov, N., Pavlyk, O., Brodtkorb, P. A., Lee, P., McGibbon, R. T., Feldbauer, R., Lewis, S., Tygier, S., Sievert, S., Vigna, S., Peterson, S., More, S., Pudlik, T., et al.: SciPy 1.0: fundamental algorithms for scientific computing in Python, Nat Methods, 17, 261–272, https://doi.org/10.1038/s41592-019-0686-2, 2020.

Wan, X. S., Sheng, H. X., Dai, M., Casciotti, K. L., Church, M. J., Zou, W., Liu, L., Shen, H., Zhou, K., Ward, B. B., and Kao, S. J.: Epipelagic nitrous oxide production offsets carbon sequestration by the biological pump, Nat Geosci, 16, 29–36, https://doi.org/10.1038/s41561-022-01090-2, 2023.

Weiss, R. F., Price, B. A., Canada, E., Rochette, P., Hutchinson, G. L., Jayasundara, S., and Wagner-Riddle, C.: Nitrous oxide solubility in water and seawater, Agric Syst, 8, 247–286, 1980.

Wilson, S. T., Ferrón, S., and Karl, D. M.: Interannual Variability of Methane and Nitrous Oxide in the North Pacific Subtropical Gyre, Geophys Res Lett, 44, 9885–9892, https://doi.org/https://doi.org/10.1002/2017GL074458, 2017.

Wu, B., Liu, F., Weiser, M. D., Ning, D., Okie, J. G., Shen, L., Li, J., Chai, B., Deng, Y., and Feng, K.: Temperature determines the diversity and structure of N_2O-reducing microbial assemblages, Funct Ecol, 32, 1867–1878, 2018.

Yang, J., Zhang, G. L., Zheng, L. X., and Zhang, F.: Seasonal variations of fluxes and distributions of dissolved N_2O in the North Yellow Sea, Huanjing Kexue/Environmental Science, 30, 2009.

Yang, S., Chang, B. X., Warner, M. J., Weber, T. S., Bourbonnais, A. M., Santoro, A. E., Kock, A., Sonnerup, R. E., Bullister, J. L., Wilson, S. T., and Bianchi, D.: Global reconstruction reduces the

https://doi.org/10.5194/egusphere-2024-4166
Preprint. Discussion started: 23 January 2025

uncertainty of oceanic nitrous oxide emissions and reveals a vigorous seasonal cycle, Proc Natl Acad Sci U S A, 117, https://doi.org/10.1073/pnas.1921914117, 2020.

Zhang, G., Zhang, J., Ren, J., Li, J., and Liu, S.: Distributions and sea-to-air fluxes of methane and nitrous oxide in the North East China Sea in summer, Mar Chem, 110, https://doi.org/10.1016/j.marchem.2008.02.005, 2008.

Zhou, J., Zheng, Y., Hou, L., An, Z., Chen, F., Liu, B., Wu, L., Qi, L., Dong, H., and Han, P.: Effects of acidification on nitrification and associated nitrous oxide emission in estuarine and coastal waters, Nat Commun, 14, 1380, 2023.

https://doi.org/10.5194/egusphere-2024-4166
Preprint. Discussion started: 23 January 2025

Figure 1: (A) Map of the stations location in the Western Mediterranean Sea Basin and (B) detailed location of the Bay of Palma (BP; blue dot) and the Cabrera National Park (CA, red dot) and Cape Ses Salines (CS; green dot) study sites. Dashed lines represent bathymetry levels. Maps were developed with the Python software version 3.12.3.

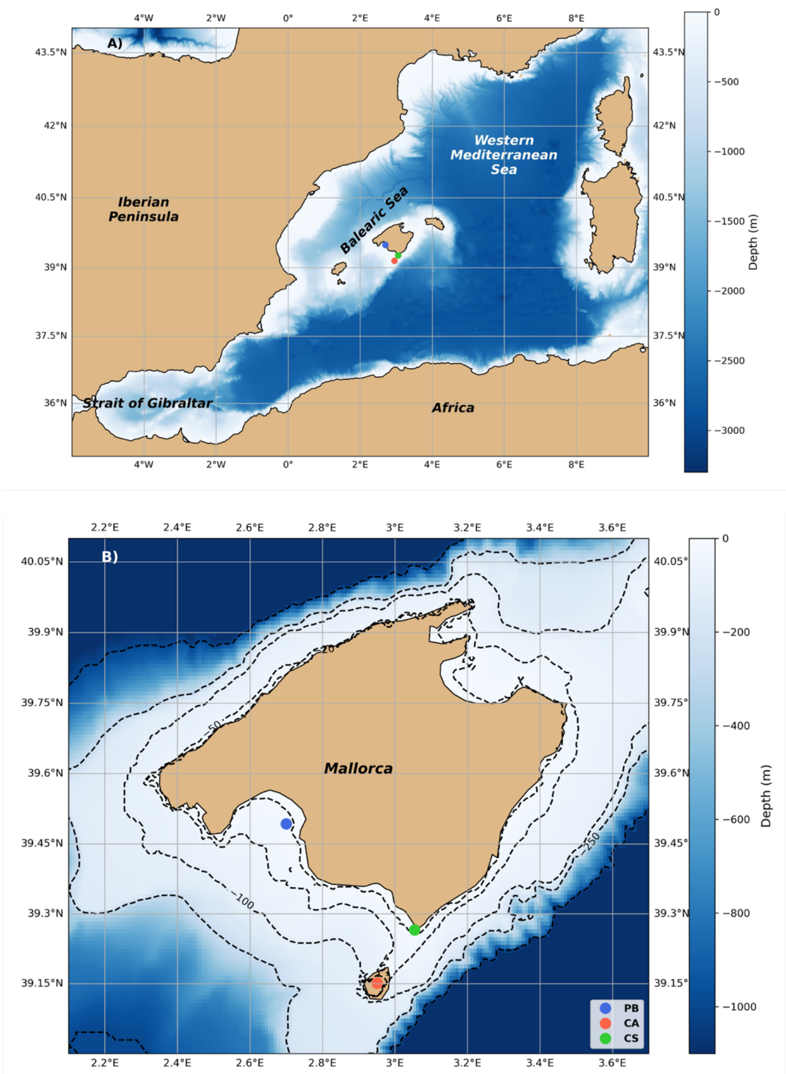

https://doi.org/10.5194/egusphere-2024-4166
Preprint. Discussion started: 23 January 2025

Figure 2: Time-series of A) Daily averaged temperature (ºC) for PB (blue dots) and CA (red dots) stations and instant values for CS site (green dots), B) Daily averaged salinity (psu) for PB (blue dots) and CA (red dots) stations and instant values for CS site (green dots) and C) Daily averaged wind speed (m s^{-1}) at 10 m height from Palma station (Spain). Figures were developed with the Python software version 3.12.3.

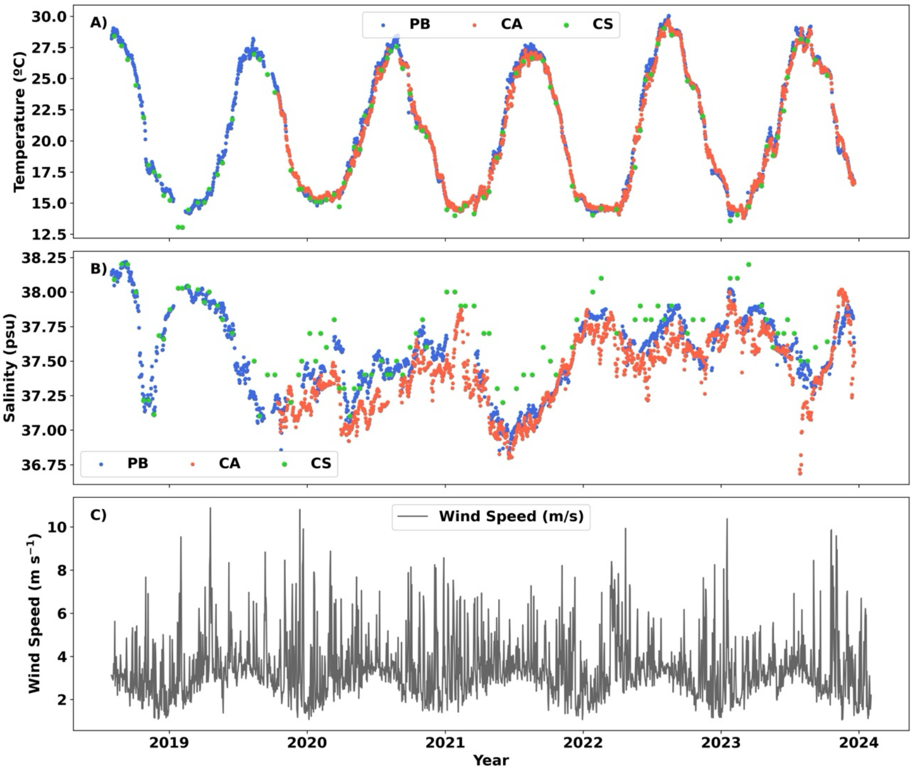

https://doi.org/10.5194/egusphere-2024-4166
Preprint. Discussion started: 23 January 2025

Figure 3: Time-series of A) Nitrous Oxide (N_2O) levels in nmol L^{-1}, B) Chlorophyll *a* (Chl *a*) in µg L^{-1}, C) Dissolved Organic Carbon (DOC) in µM, D) Dissolved Oxygen (DO) in µmol Kg^{-1}, E) Nitrate (NO_3^-) in µM and F) Nitrite (NO_2^-) in µM measured in the samples collected in BP (blue dots), CA (red dots) and CS (green dots). Figures were developed with the Python software version 3.12.3.

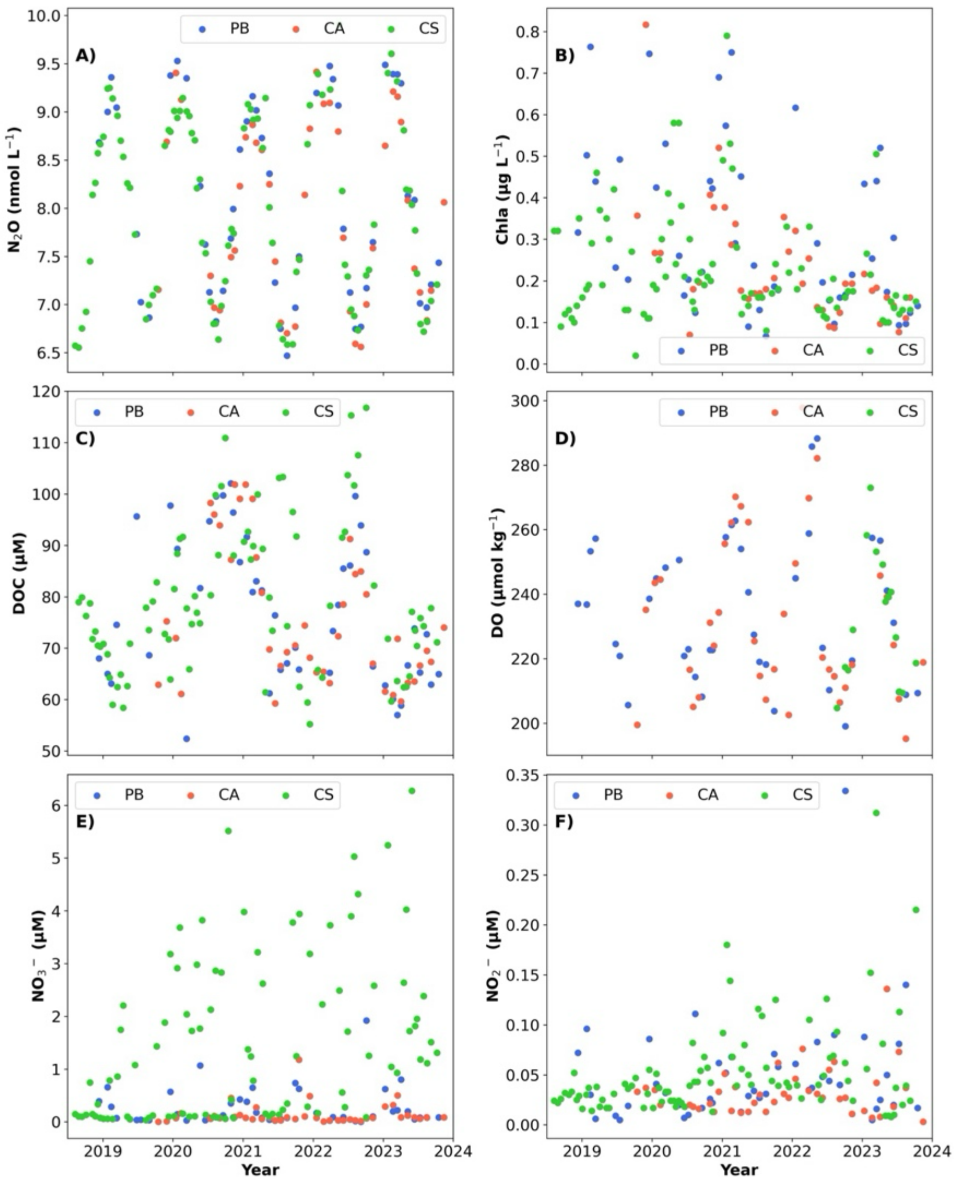

https://doi.org/10.5194/egusphere-2024-4166
Preprint. Discussion started: 23 January 2025

Figure 4: The relative importance of the leading environmental and biogeochemical variables driving the nitrous oxide variability analyzed through cross-valued boosting (CVB). These are, in decreasing order: Temperature, Chlorophyll *a* (Chla), Salinity, Dissolved Organic Carbon (DOC), Nitrate (NO_3) and Nitrite (NO_2). The figure was developed using Python software version 3.12.3.

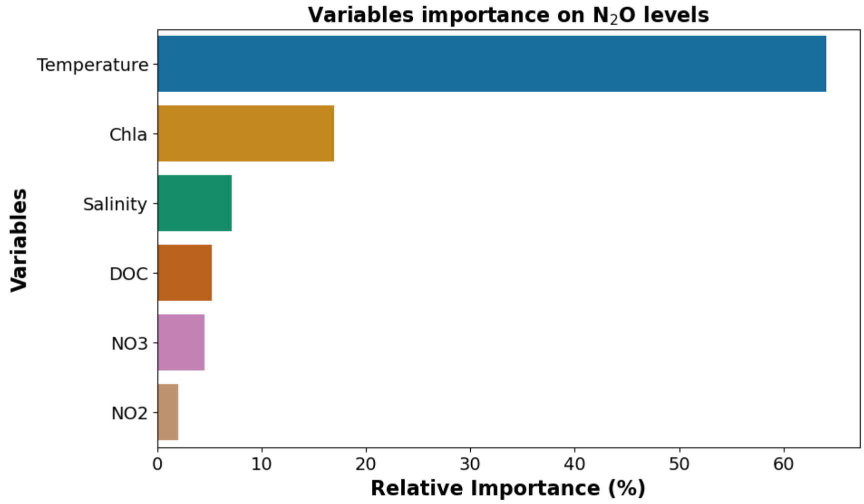

https://doi.org/10.5194/egusphere-2024-4166
Preprint. Discussion started: 23 January 2025

Figure 5: Linear relation of Temperature (ºC) with Saturation Percentage of N_2O (Sat%N_2O) levels in percentage from the data obtained in BP (blue dots), CA (red dots) and CS (green dots). Linear equations are represented in blue for PB, red for CA and green for CS stations. Figures were developed with the Python software version 3.12.3.

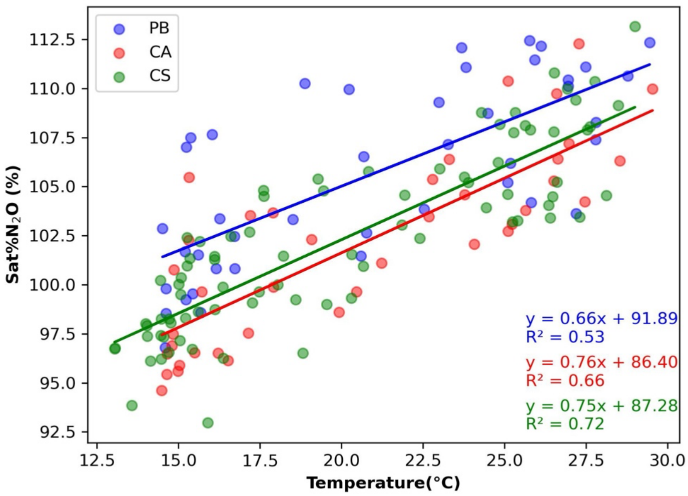

https://doi.org/10.5194/egusphere-2024-4166
Preprint. Discussion started: 23 January 2025

Figure 6: Box plot of monthly averaged values of air-sea Nitrous Oxide (N_2O) transfer (FN_2O) in µmol m^{-2} d^{-1} for all the study years (left axis) and averaged temperature (ºC) values (right axis; grey line) for the PB (upper plot), CA (middle plot) and CS (lower plot) sites. Error bars represent ± standard deviation. Figures were developed with the Python software version 3.12.3.

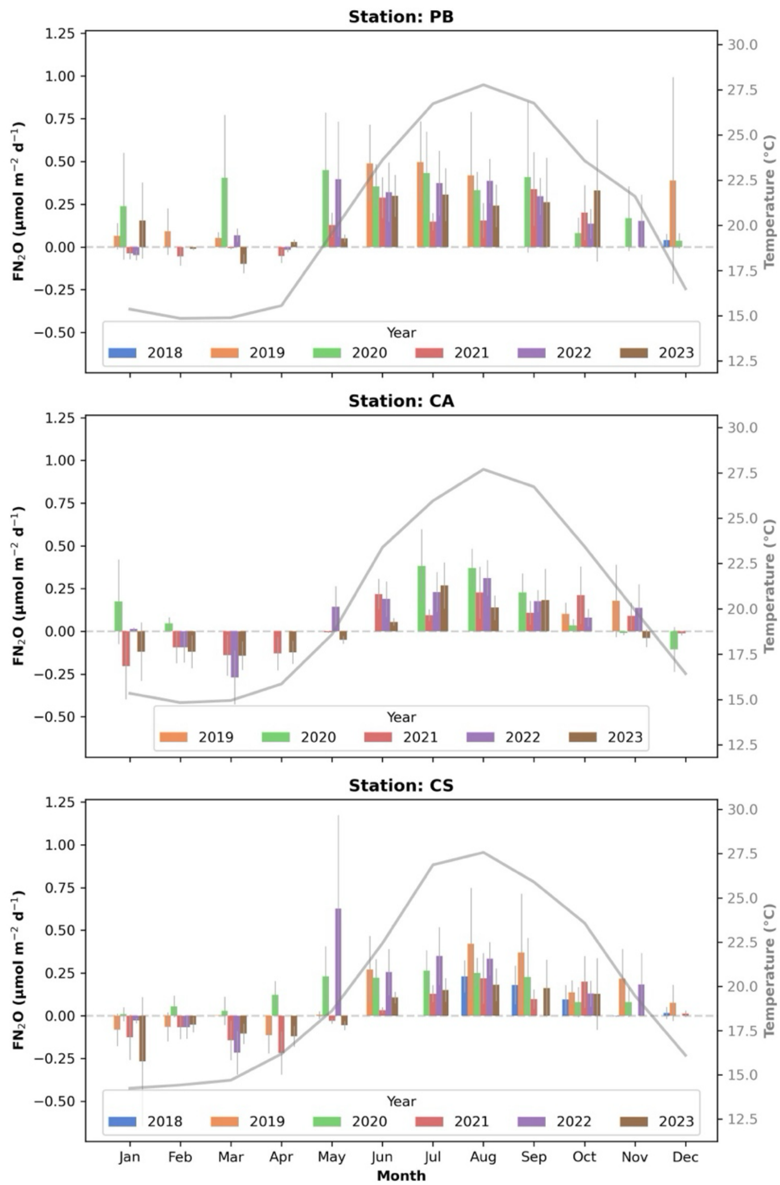

https://doi.org/10.5194/egusphere-2024-4166
Preprint. Discussion started: 23 January 2025

Table 1: Seasonally averaged values of Temperature(ºC), Salinity (PSU), Chlorophyll a (Chl a; µg L^{-1}), Dissolved Oxygen (DO; µmol Kg^{-1}), Apparent Oxygen Utilization (AOU; µmol Kg^{-1}), Nitrate^{-}(µM), Nitrite (µM), Silicate (µM), Dissolved Organic Carbon (DOC; µM), N_2O (nmol), % saturation N_2O measured in the samples collected in BP (Buoy of Palma), CA (Cabrera National Park) and CS (Cape Ses Salines). Variability is represented as ± standard deviation. * DO data is only available from August 2022 at the CS station.

	BP (n = 48)				CA (n = 42)				CS (n =91)			
	Winter	**Spring**	**Summer**	**Fall**	**Winter**	**Spring**	**Summer**	**Fall**	**Winter**	**Spring**	**Summer**	**Fall**
Temperature (ºC)	15.5± 0.8	16.6± 2.3	26.0± 2.0	24.5± 2.6	15.3± 0.9	16.5± 1.9	25.9± 2.0	23.1± 3.3	14.9± 1.0	16.9± 1.9	25.7± 2.5	23.0± 2.9
Salinity (psu)	37.6± 0.2	37.7± 0.3	37.4± 0.2	37.5± 0.2	37.6± 0.2	37.4± 0.2	37.3± 0.3	37.4± 0.2	37.8± 0.2	37.7± 0.3	37.6± 0.3	37.6± 0.3
Chl *a* (µg L^{-1})	0.6± 0.2	0.3± 0.1	0.2± 0.1	0.2± 0.1	0.3± 0.1	0.2± 0.1	0.1± 0.0	0.3± 0.2	0.3± 0.2	0.3± 0.2	0.2± 0.1	0.2± 0.1
DO (µmol Kg^{-1})	246.7± 10.1	258.5± 15.7	218.1± 7.4	211.5± 9.0	248.7± 26.8	262.4± 15.0	213.4± 9.0	218.4± 11.8	265.6± 10.4*	244.0± 6.8*	212.6± 9.6*	220.4± 5.8*
AOU (µmol Kg^{-1})	-5.5± 7.9	-23.0±16.1	-17.8± 5.3	-5.4± 5.5	-6.6± 24.8	-26.5± 13.5	-12.4± 6.9	-6.5± 7.4	-17.3± 12.1*	-13.9± 4.0*	-16.7± 4.9*	-13.9± 2.3*
Nitrate (µM)	0.2± 0.4	0.2± 0.3	0.1± 0.0	0.4± 0.6	0.2± 0.2	0.1± 0.2	0.1± 0.0	0.2± 0.3	1.4± 1.6	1.9± 1.6	1.4± 1.5	1.4± 1.5
Nitrite (µM)	0.06± 0.03	0.03± 0.02	0.05± 0.04	0.07± 0.1	0.03± 0.02	0.04± 0.04	0.03± 0.02	0.03± 0.02	0.05± 0.05	0.05± 0.06	0.05± 0.03	0.05± 0.04
Silicate (µM)	2.9± 2.8	4.4± 3.6	6.7± 5.5	8.1± 5.3	4.0± 3.1	3.1± 2.3	7.6± 6.8	5.1± 3.9	0.9± 0.9	2.0± 2.6	1.4± 1.7	0.8± 0.9
DOC (µM)	76.5± 14.2	65.9± 10.7	80.8± 13.2	81.1± 16.3	75.4± 17.3	71.0± 9.5	76.6± 13.8	78.3± 11.7	74.0± 12.6	71.8± 10.5	88.0± 14.3	84.1± 14.4
N_2O (nmol L^{-1})	9.2± 0.3	9.0± 0.5	7.20± 0.5	7.4± 0.4	9.0± 0.4	8.7± 0.4	7.1± 0.3	7.4± 0.6	9.0± 0.3	8.7± 0.5	7.1± 0.5	7.4± 0.5
N_2O saturation (%)	101.8± 3.3	102.6±4.4	109.6± 2.8	107.3± 3.2	98.6± 3.4	97.9± 2.7	106.6± 3.2	103.8± 3.0	99.0±2.0	100.1± 4.9	106.9± 2.9	104.6± 2.5

https://doi.org/10.5194/egusphere-2024-4166
Preprint. Discussion started: 23 January 2025

Table 2: Annual N_2O flux (µmol m^{-2} y^{-1}) per station since 2019 for PB (Buoy of Palma) and CS (Cape Ses Salines) station and from 2020 for CA (Cabrera National Park) site. Variability is represented as ± standard deviation.

Annual N_2O flux per station (µmol m^{-2} y^{-1})					
	2019	**2020**	**2021**	**2022**	**2023**
PB	117.1 ± 59.2	111.1 ± 51.8	36.8 ± 48.4	64.7 ± 61.4	61.0± 51.5
CA	N/A	71.0 ± 61.1	11.2 ± 54.8	26.2 ± 58.9	0.1± 51.0
CS	36.6 ± 70.9	49.7 ± 40.5	1.9 ± 54.3	63.2 ± 73.8	7.6 ± 48.5